J. S. Afr. Inst. Min. Metall., vol. 90, no. 11.
Nov. 1990. pp. 289-301.

The washability of fine South African coals

by R.P. KING* and N. BIRTEK*

SYNOPSIS

The washability characteristics of fine South African coals were measured and were found to be well characterized by an M-curve having the equation $Z = aQ^b \exp(cQ) \times dQ$, where Z is the ash content per 100 units of total feed and Q is the mass yield. Parameters a, b, c, and d were determined for 23 different samples of coal from important coal seams in the main South African coalfields in the size range 0,0025 to 1 mm. The relationship between ash content and relative density was determined and correlated by means of two linear relationships. This characteristic behaviour was explained in terms of the liberation of macerals and the different association between the mineral matter and the two major macerals vitrinite and inertinite. The results obtained in this study can be used to calculate the expected performance of an ideal separation process, and can also be used as input for the simulation of real beneficiation plants. An example is worked through in detail to illustrate the method of calculation.

SAMEVATTING

Die wasbaarheidseienskappe van Suid-Afrikaanse fynsteenkool is gemeet an daar is gevind dat hulle goed gekarakteriseer word deur 'n M-kromme met die vergelyking $Z = aQ^b \exp(cQ) \times dQ$ waar Z die asinhoud per 100 eenhede van die totale toevoer en Q die massaopbrengs is. Die parameters a, b, c en d is vir 23 verskillende steenkoolmonsters afkomstig van belangrike steenkoollae in die vernaamste Suid-Afrikaanse steenkoolvelde, in die groottestrek 0,0025 tot 1 mm, gemeet. Die verhouding tussen die asinhoud en relatiewe digtheid is bepaal en deur middel van twee lineêre verhoudings gekorreleer. Hierdie kenmerkende gedrag is in terme van die bevryding van maserale en die verskillende assosiasie tussen die mineraalstof en die twee vernaamste maserale vitriniet en inertiniet verklaar. Die resultate wat in hierdie studie verkry is, kan gebruik word om die verwagte werkverrigting van 'n ideale skeidingsproses te bereken, en ook as invoer vir die simulasie van werklike veredelingsaanlegte. 'n Voorbeeld word in besonderhede uitgewerk om die berekeningsmetode te illustreer.

Introduction

The washability characteristics of coal constitute essential information for the coal-processing engineer if he is to correctly and effectively assess the performance of a coal-washing plant. Although the washability characteristics of coals from South African collieries are well known at coarser sizes, this information is almost entirely lacking in the size range below about 1 mm. This is a serious omission since fairly large quantities of fines are produced in South African collieries and washeries, and there is considerable economic incentive to consider beneficiation of this material.

South African coals are, for the most part, fairly difficult to beneficiate because of their unfavourable washability characteristics. Conventional mineral-processing wisdom dictates that finer grinding should improve the liberation of ash, and therefore should improve the washability, and simplify and improve the processing technology.

These observations led to a major investigation in the Department of Metallurgy and Materials Engineering at the University of the Witwatersrand of the washability of a variety of samples of fine coal taken from a representative selection of coal seams and coalfields in South Africa. The object of this investigation was to determine the washability characteristics at sizes finer than 1 mm, and to determine whether ash-forming minerals can be liberated by size reduction. This paper reports the results of this investigation.

* Department of Metallurgy and Minerals Engineering, University of the Witwatersrand, P.O. Wits, 2050 Transvaal.

 SA ISSN 0038-223X/3.00 + 0.00. Paper received 24th July, 1989. Modified paper received 20th June, 1990.

Coal Used in This Study

Samples of coal were obtained from a number of operating collieries in most of the South African coalfields (Table I). The samples were carefully collected and prepared to produce fine material for particle-size analysis, float-and-sink analysis, and petrographic analysis. The sampling and sample preparation are described and analysed in detail elsewhere[2].

After appropriate samples had been crushed to smaller than 1 mm, the material was split into narrow size fractions by sieving. These fractions were subjected to float-and-sink analysis, and the ash content of each size fraction was determined by the use of standard techniques. The ash content of individual float-sink fractions was also determined.

Particular care was taken to ensure the accuracy of the float-and-sink procedure, a sequential two-stage procedure being adopted. This procedure is particularly appropriate for fine particles, and has been developed to a high level of accuracy and reproducibility in the Department's laboratory. Details of the procedure, with a detailed statistical analysis of the sources of error, are given elsewhere[2].

Washability Results

The results collected during this study are too voluminous to be included in full in this paper. Here, only selected results are presented in graphical and tabular form to illustrate the main features. The complete results are readily available in other documents[2-4].

The washability results for sample 9 for the size fractions minus 425 plus 300 μm and minus 38 plus 25 μm are given in Table II, and are shown graphically in Fig. 1. The M-curve was used for illustration in preference to

TABLE I
ORIGIN OF THE COAL SAMPLES

Sample no.	Sample designation	Coalfield	Colliery	Seam	Band in seam
1	NEM2 B6*	Witbank	Springbok	2	B
2	NEM2 C12*	Witbank	Springbok	2	C
3	NEM2 D16*	Witbank	Springbok	2	D
4	NEM2 D18*	Witbank	Springbok	2	D
5	Matla†		Matla	?	?
6	Waterberg†	Waterberg		?	?
7	Wit 4 upper	Witbank	Eikeboom	4	Upper
8	Wit 4 lower	Witbank	Eikeboom	4	Lower
9	Wit 2 top	Witbank	Eikeboom	2	D
10	Wit 2 middle	Witbank	Eikeboom	2	C
11	Wit 2 bottom	Witbank	Eikeboom	2	B
12	Wit 1	Witbank	Eikeboom	1	–
13	Tshin	Soutpansberg	Tshinkondeni	Top	Lower 6 bands
14	Secunda	Highveld	Middlebult	4	–
15	Sigma 2A	Vereeniging–Sasolburg	Sigma	2	A
16	Sigma 2B	Vereeniging–Sasolburg	Sigma	2	B
17	Sigma 3	Vereeniging–Sasolburg	Sigma	3	–
18	Usutu B	Eastern Transvaal		B	–
19	Usutu C L	Eastern Transvaal		C	Lower
20	Usutu C L	Eastern Transvaal		C	Upper
21	Groot 4	Waterberg	Grootegeluk	Zone 10	Sample 4
22	Groot 11	Waterberg	Grootegeluk	Zone 8	Sample 11
23	Groot 18	Waterberg	Grootegeluk	Zone 7	Sample 18

* These samples were originally obtained during an earlier coal-characterization project. The material in these samples has been comprehensively characterized[1].
† Samples supplied by Sasol. Their precise origins are not known.

the rather more conventional densiometric curve because useful operating information, such as the yields and product quality to be expected from ideal washing operations, can be deduced more easily from the M-curve. In addition, the M-curve provides effective graphical procedures for the optimization of plant flowsheets that include flotation, as well as gravity-separation, unit operations[5].

The geometry of the M-curve is illustrated in Fig. 2. This representation shows the cumulative recovery of ash in an ideal densiometric separation normalized with respect to the mass of total sample plotted against the yield of total solids. Clearly, the density of separation increases from left to right along the curve. The utility of the M-curve results from its vectorial character. For example, with reference to Fig. 2, consider a single-stage separation process that separates at point F and gives two products represented by lines AF and FB. The ash content of the light product is given by the slope of line AF, and that of the heavy product by the slope of line FB. The ash content of the light product at the separation density (this is the heaviest material that will float at the separation density) is given by the slope of the tangent to the M-curve at point F. If the separation point is chosen so that this tangent is parallel to the feed line, then the separation efficiency of the washing unit will be maximized[6]. These geometrical properties are widely known and used by coal-processing engineers.

Not so well known is the property of the M-curve that shows the state of liberation of the sample material. If the liberation between organic macerals and ash-forming minerals were perfect and complete, the M-curve would consist of two straight lines such as AC and CB. AC would represent the maceral material containing no ash (thus zero slope), and line CB would represent the ash minerals (slope 1,0). This ideal is never achieved, and actual M-curves have the curved shape shown in Fig. 1. However, the further the curve bends into corner ACB, the greater the separation of ash-forming minerals from the coal macerals. This is illustrated by the sequence of three curves in Fig. 2.

From all the coals studied in this project, it was not possible to produce entirely ash-free particles even at the lowest relative density of separation. This is reflected in the non-zero slope of the M-curve at the origin that was always observed. Likewise, it was never possible to produce carbon-free mineral particles that would represent perfectly liberated mineral matter. As it was impossible to specify the liberation of macerals or mineral matter in the conventional way, use was made of a liberation index that reflects both the liberation characteristics and the potential for the clean separation of macerals from mineral matter. This liberation index is defined as the ratio of the area AFBA to the triangular area ACBA in Fig. 2 and ranges from 0 to 1, depending on the degree of separation of the macerals from the mineral matter. Coal that has a liberation index close to 1 is well separated and can easily be washed to form a low-ash clean coal, and *vice versa*.

The liberation index also shows effectively how the liberation, or separation of macerals from mineral matter, improves as the particle size decreases. This can be seen in Fig. 1, in which the sample containing the smaller particles shows the greater curvature. The liberation index

TABLE II
WASHABILITY AND REALEASE DATA FOR SAMPLE 9
(WITBANK NO. 2 SEAM TOP, −425 +300 μm FRACTION)

Relative density of separation	Mean relative density	Specific volume	Floats					Sinks	
			Mass fraction %	Ash fraction %	Cumulative mass %	Ash per 100 units of feed	Cumulative ash %	Cumulative mass %	Cumulative ash %
1,301	1,280	0,782	0,6	1,30	0,6	0,0001	1,30	100,0	11,72
1,344	1,322	0,756	2,6	2,25	3,2	0,0007	2,07	99,4	11,78
1,377	1,360	0,735	1,5	3,26	4,7	0,0012	2,45	96,8	12,04
1,418	1,398	0,716	4,8	4,12	9,5	0,0031	3,29	95,3	12,18
1,459	1,438	0,695	5,3	4,66	14,8	0,0056	3,78	90,5	12,60
1,492	1,475	0,678	19,6	5,58	34,4	0,0165	4,81	85,2	13,10
1,535	1,513	0,661	34,3	8,33	68,7	0,0451	6,57	65,6	15,34
1,584	1,559	0,641	16,0	12,50	84,7	0,0651	7,69	31,3	23,03
1,618	1,601	0,625	3,0	15,48	87,7	0,0698	7,95	15,3	34,03
1,644	1,631	0,613	3,4	18,20	91,1	0,0759	8,34	12,3	38,56
1,694	1,669	0,599	2,1	21,82	93,2	0,0805	8,64	8,9	46,34
1,779	1,736	0,576	1,3	27,92	94,5	0,0842	8,90	6,8	53,91
1,999	1,889	0,529	0,6	40,78	95,1	0,0866	9,11	5,5	60,05
2,460	2,233	0,448	1,5	70,19	96,6	0,0971	10,05	4,9	62,41
−2,460	–	–	3,4	58,98	100,0	0,1172	11,72	3,4	58,98
Total			100,0						

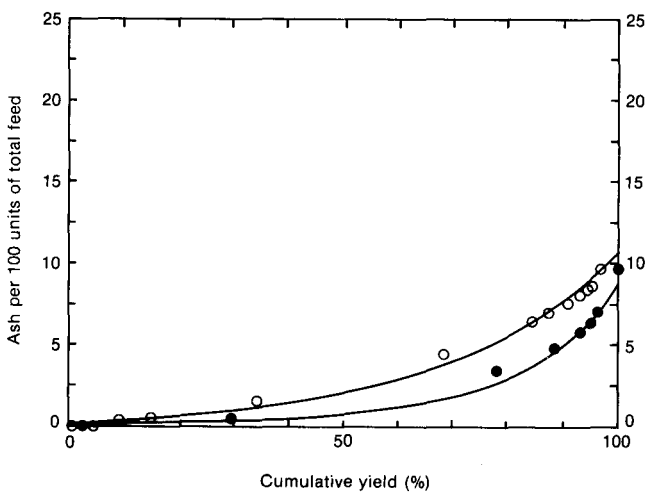

Fig. 1—Washability data of fine coal from Witbank No. 2 seam top represented as the M-curve. ○ −425 +300 μm size fraction. ● −38 +25 μm size fraction

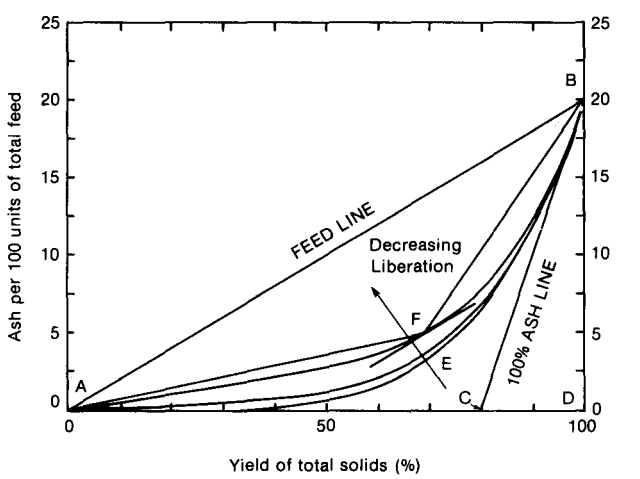

Fig. 2—Geometrical characteristics of the M-curves for coal containing 20 per cent ash and exhibiting varying degrees of liberation

removes the effect of the variable ash content of feed material.

The M-curves for all the materials studied were found to fit an empirical curve of the form

$$Z = aQ^b \exp(cQ) + dQ, \quad \ldots\ldots (1)$$

where Z is the ash content per 100 units of total feed, Q is the mass yield, and a, b, c, and d are constants. The constants are not independent since the M-curve must satisfy the relationship $Z = f$ at $Q = 1{,}0$, where f is the ash content of the feed sample.

Thus, $f = a\exp(c)$. ..... (2)

The analytical form for the M-curve is useful, and the following quantities are easy to obtain:

The ash content of light product at yield Q:

$$a_c = \frac{Z}{Q} = aQ^{b-1} \exp(cQ) + d. \quad \ldots\ldots (3)$$

The instantaneous ash content at the separation density:

$$a_I = \frac{dZ}{dQ} = aQ^{b-1} \exp(cQ)\,(b + cQ) + d. \quad \ldots\ldots (4)$$

The limiting ash content at low density:

$$a_L = \frac{dZ}{dQ} \text{ at } Q = 0$$

$$= d. \quad \ldots\ldots (5)$$

The liberation index is given by

$$LI = \frac{0{,}5f - \int_0^1 Z\,dQ}{0{,}5f - 0{,}5f^2}$$

$$= \frac{f - 2ac^{(b+1)} \int_0^c t^b \exp(t)\,dt - d}{f - f^2} \quad \ldots\ldots (6)$$

A comparison between the experimental data and equation (1) is shown in Fig. 1. The fitted values of the para-

meters *a*, *b*, *c*, and *d* are given for some of the samples studied in Tables III and IV. Values for the liberation index and the increase in the liberation index between the larger size and the smaller size are also given. These parameters were used in the construction of the washability curves for all the coals studied.

TABLE III
M-CURVE REGRESSION PARAMETERS AND LIBERATION INDICES

Sample	Size μm	Constants				Liberation index
		a	*b*	*c*	*d*	
	−1000	0,00203	1,0000	3,649	0,0215	52,1
NEM 2	−500+425	0,00322	1,0000	3,117	0,0191	48,4
	−300+250	0,00191	1,0000	3,636	0,0208	51,2
B 6	−150+125	0,00175	1,0000	3,832	0,0141	57,5
	−90+75	0,00083	1,0000	4,565	0,0173	61,7
	−1000	0,00582	1,0000	2,751	0,040	41,6
NEM 2	−500+425	0,00749	1,0000	2,366	0,045	35,0
	−300+250	0,00929	1,0000	2,201	0,040	35,4
C 12	−150+125	0,00741	1,0000	2,241	0,035	34,4
	−90+75	0,00463	1,0000	2,980	0,035	44,9
	−1000	0,01438	1,0000	2,016	0,0322	38,9
NEM 2	−500+425	0,01579	1,0000	1,896	0,0324	37,0
	−300+250	0,01328	1,0000	2,064	0,0331	38,8
D 16	−150+125	0,01006	1,0000	2,347	0,0294	43,0
	−90+75	0,00658	1,0000	2,382	0,0288	38,0
	−1000	0,01151	1,0000	2,382	0,0288	46,1
NEM 2	−500+425	0,01518	1,0000	2,104	0,0227	44,2
	−300+250	0,01406	1,0000	2,195	0,0192	46,5
D 18	−150+125	0,01171	1,0000	2,373	0,0298	45,9
	−90+75	0,00953	1,0000	2,453	0,0234	46,6
	−1000	0,00099	1,0000	4,937	0,0306	66,6
	−500+425	0,00131	1,0000	4,124	0,0300	51,8
Matla	−300+250	0,00078	1,0000	4,801	0,0240	60,6
	−150+125	0,00050	1,0000	5,497	0,0190	70,7
	−90+75	0,00037	1,0000	6,102	0,0230	78,5
	−1000	0,12103	2,6694	0,431	0,0310	54,9
	−500+425	0,04256	1,6846	1,598	0,0180	58,8
Waterberg	−300+250	0,04547	1,9483	1,508	0,0161	61,7
	−150+125	0,50921	5,1811	−1,048	0,0450	64,0
	−90+75	0,01588	2,1181	2,393	0,0192	67,8

Ash Content

The washability results presented in the previous section were determined in terms of particle ash content. However, in gravity-separation operations, it is the particle relative density that determines the separation characteristics. It is therefore necessary to examine the relationship between ash content and particle relative density. In general, the relative density of a particle increases as the ash content increases, but the precise form of the relationship has never been investigated for coal.

The ash content of the individual washability fractions from the float-and-sink analysis was determined. Because of the very narrow range of the successive float fractions (approximately 0,04 relative density units), the measured ash content could be assigned to particles having the average relative density of the sample.

If a coal particle can be considered to consist of two phases, organic and mineral matter, then a simple analysis shows that the ash content should be a linear function of the specific volume (reciprocal of particle density) of the particle. If ρ represents the density of the particle, ρ_m the density of the mineral matter, and ρ_o the density of the organic matter, then

$$\frac{1}{\rho} = \frac{m_m}{\rho_m} + \frac{m_o}{\rho_o}, \quad \text{..... (7)}$$

where m_m is the mass fraction of the mineral matter and m_o the mass fraction of the organic matter. If the ash content of the mineral matter is a_m (this is approximately 83 per cent for most South African coals), then the ash content of the particle is given by

$$\% \text{ ash} = a_m m_m = \frac{a_m}{1/\rho_m - 1/\rho_o}\left(\frac{1}{\rho} - \frac{1}{\rho_o}\right)$$
$$= A(1/\rho) + B. \quad \text{..... (8)}$$

Thus, for a two-phase system, the ash content can be expected to vary linearly with the specific volume of the particle. The results for one sample tested are shown as plots of percentage ash against the reciprocals of relative density in Fig. 3.

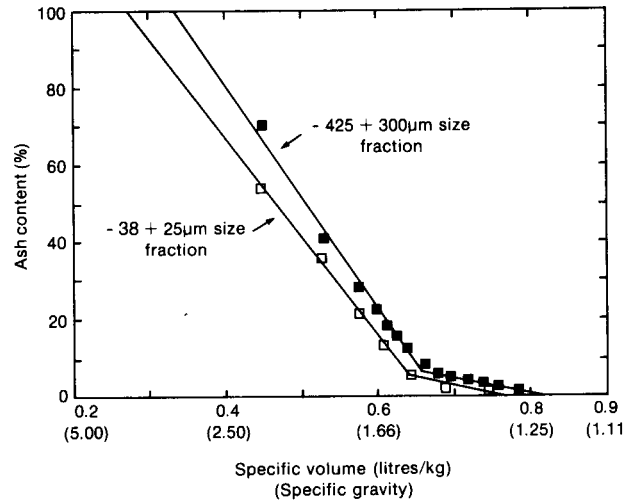

Fig. 3—Ash content as a function of specific volume for coal from Witbank No. 2 seam top. The straight lines follow equation (8)

All the results that were analysed in this study showed the same characteristics when plotted in this way: two straight lines with a distinct break point. In some samples such as the Witbank No. 2 and Usutu C Upper, the lower line was well-defined, extending over a significant range of specific volume. In other samples, the lower line was ill-defined, such as in Fig. 4. This behaviour is distinct and represents a definite characteristic behaviour of South African coals. For ease of analysis, two straight lines were fitted to each of the experimental plots, although the straight line for the lower points has no theoretical significance when there are fewer than three points on this portion of the curve. However, the representation by means of two straight lines is very convenient for practical use. Once the relationship has been established, it is possible to determine the ash content for any washability fraction of the coal. For some of the samples, the constants for the slope and intercept of these lines are given in Tables V and VI.

TABLE IV
M-CURVE REGRESSION PARAMETERS AND LIBERATION INDICES

Sample	Size μm	Constants				Liberation index	Difference
		a	*b*	*c*	*d*		
Witbank N4 up	−425+300	0,03190	1,0000	2,140	0,0197	59,2	
Witbank N4 up	−38+25	0,00663	1,0000	3,791	0,0288	81,8	22,6
Witbank N4 low	−425+300	0,01229	1,0000	2,236	0,0167	46,5	
Witbank N4 low	−38+25	0,00064	1,0000	4,971	0,0075	69,7	23,2
Witbank N2 top	−425+300	0,00766	1,0000	2,499	0,0130	48,5	
Witbank N2 top	−38+25	0,00033	1,0000	5,489	0,0113	67,6	19,1
Witbank N2 mid	−425+300	0,00987	1,0000	2,374	0,0142	48,0	
Witbank N2 mid	−38+25	0,00006	1,0000	7,674	0,0232	77,3	29,3
Witbank N2 bot	−425+300	0,03602	1,2281	0,831	0,0133	28,0	
Witbank N2 bot	−38+25	0,00367	1,0000	2,914	0,0200	45,4	17,4
Witbank N1	−425+300	0,02233	1,0000	1,301	0,0090	32,0	
Witbank N1	−38+25	0,00325	1,0000	2,974	0,0105	50,2	18,2
Tshinkondeni	−1000+25	0,00653	1,0000	3,102	0,0178	58,9	
Tshinkondeni	−38+25	0,01821	2,5305	2,256	0,0202	70,1	11,2
Secunda	−1000+25	0,01933	1,0000	2,095	0,0274	46,4	
Secunda	−38+25	0,00413	1,2398	3,587	0,0414	59,5	13,1
Sigma 2A	−425+300	0,24203	1,7914	0,307	0,0226	48,7	
Sigma 2A	−38+25	1,21499	3,4116	−1,486	0,0521	48,3	−0,4
Sigma 2B	−425+300	0,25132	1,8312	0,235	0,0351	46,6	
Sigma 2B	−38+25	20,73030	5,4334	−4,189	0,0628	48,7	2,1
Sigma 3	−425+300	0,10586	1,5903	0,888	0,0262	49,0	
Sigma 3	−38+25	0,12727	1,9654	0,621	0,0464	48,9	−0,1
Usutu B	−425+300	0,02392	1,0000	1,930	0,0256	45,2	
Usutu B	−38+25	0,17367	4,1755	−0,022	0,0444	61,8	16,6
Usutu C up	−425+300	0,06801	1,4522	1,045	0,0430	41,0	
Usutu C up	−38+25	0,03925	1,4456	1,689	0,0328	53,7	12,7
Usutu C low	−425+300	0,00455	1,0000	3,297	0,0288	54,5	
Usutu C low	−38+25	0,27390	5,3149	−0,144	0,0393	80,3	25,8
Groot. 4	−425+300	0,05113	1,7299	1,441	0,0130	59,0	
Groot. 4	−38+25	0,13479	3,0453	0,650	0,0093	74,2	15,2
Groot. 11	−425+300	0,34900	2,4946	−0,129	0,0124	58,0	
Groot. 11	−38+25	5,34396	5,6138	−2,917	0,0328	69,7	11,7
Groot. 18	−425+300	0,02917	1,1820	2,053	0,0124	58,6	
Groot. 18	−38+25	22,04043	7,1635	−4,411	0,0445	69,2	10,4

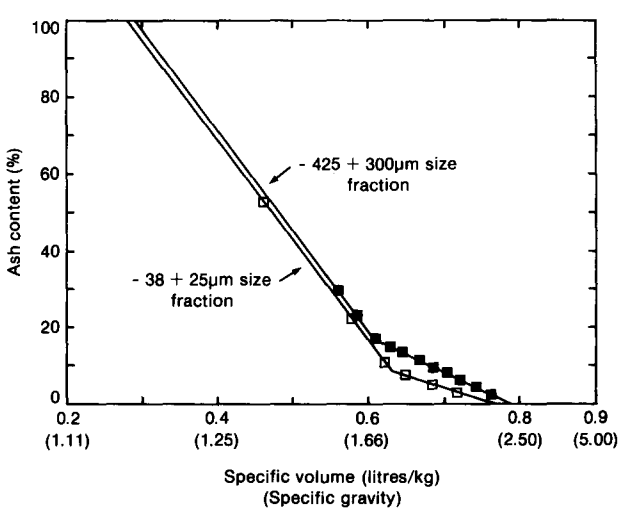

Fig. 4—Ash content as a function of specific volume for coal from the Eastern Transvaal coalfield (Usutu seam C upper). The straight lines follow Equation (8)

The nature of this relationship between ash content and particle specific volume can be explained in the following way. Equation (8) represents this relationship for a two-phase system and shows that the straight line should pass through a point ρ_m at an ash content of 100 per cent that has abscissa equal to the specific volume of the mineral matter (Fig. 5). This line should also pass through the point S at 0 per cent ash, which has abscissa equal to the specific volume of the organic phase.

Each point on the lower line represents a single point on a similar straight line but, for each of these points, the relative density of the organic phase becomes progressively lower as the points drift towards point R in Fig. 5. Thus, these points represent coal particles with lighter and lighter macerals, but all include mineral matter with a relative density defined by point ρ_m. These lines are shown as broken lines in Fig. 5.

In all the coals studied, the two dominant macerals observed were vitrinite and inertinite, with only very small amounts of exinite. It appears that, as the particles

TABLE V

PARAMETERS IN EQUATION (8) FOR PERCENTAGE ASH AS A FUNCTION OF PARTICLE SPECIFIC VOLUME

Sample	Size μm	N	A (−)	B	Corr. coeff. (−)	95% conf. lim. A±	95% conf. lim. B±	N1	A1 (−)	B1	Corr. coeff. (−)	95% conf. lim. A1±	95% conf. lim. B1±
	−1000	5	0,4872	0,3989	0,9887	0,1352	0,0997	6	2,5381	1,8096	0,9993	0,1327	0,0842
NEM	−500+425	5	0,7119	0,5703	0,9906	0,1806	0,1330	6	2,4488	1,7320	0,9979	0,2202	0,1512
	−300+250	5	0,6360	0,5119	0,9788	0,2443	0,1799	6	2,3975	1,7367	0,9996	0,1478	0,0913
B 6	−150+125	5	0,6210	0,4936	0,9815	0,2222	0,1636	6	2,5214	1,8089	0,9991	0,1478	0,0940
	−90+75	4	0,3125	0,2598	0,9853	0,1649	0,1136	7	2,4657	1,770	0,9988	0,1419	0,0913
	−1000	5	1,3138	0,9809	0,9792	0,4993	0,3380	3	4,8700	3,2259	0,9989	2,8932	1,7659
NEM	−500+425	5	0,9878	0,7679	0,9356	0,6845	0,4741	3	2,4235	1,7092	0,9937	3,4712	2,1729
	−300+250	5	1,0127	0,7823	0,9334	0,7152	0,4967	3	2,4138	1,7008	0,9974	2,2312	1,3965
C 12	−150+125	5	0,2469	0,2291	0,9278	0,3020	0,2196	6	1,9492	1,4068	0,9970	0,2094	0,1321
	−90+75	5	0,5146	0,4246	0,9193	0,4047	0,2901	5	2,2463	1,6046	0,9917	0,5334	0,3339
	−1000	6	1,1119	0,8999	0,9973	0,1139	0,0829	5	1,6565	1,2908	0,9888	0,4585	0,2870
NEM	−500+425	6	1,1377	0,9230	0,9963	0,1367	0,0995	5	1,4285	1,1427	0,9859	0,4458	0,2893
	−300+250	7	1,3032	1,0383	0,9928	0,1813	0,1302	4	1,3430	1,0927	0,9985	0,2238	0,2385
D 16	−150+125	5	0,9339	0,7610	0,9902	0,2417	0,1784	6	2,1218	1,5752	0,9959	0,2667	0,1692
	−90+75	5	0,9069	0,7360	0,9926	0,2033	0,1497	6	2,1399	1,5844	0,9946	0,3086	0,1960
	−1000	6	0,8669	0,6987	0,9929	0,1434	0,1043	5	2,8558	2,0394	0,9989	0,2516	0,1574
NEM	−500+425	5	1,0416	0,8148	0,9995	0,0592	0,0437	6	2,8704	2,0817	0,9990	0,1820	0,1153
	−300+250	5	0,9256	0,7453	0,9985	0,0807	0,0596	6	2,8149	2,0366	0,9995	0,1247	0,0790
D 18	−150+125	5	0,7933	0,6414	0,9985	0,0807	0,0596	6	2,5500	1,8511	0,9993	0,1370	0,0874
	−90+75	5	0,8203	0,6584	0,9932	0,1760	0,1297	6	2,8941	2,0712	0,9978	0,2659	0,1690
	−1000	2	0,9867	0,7675	0,9976	–	–	10	2,4384	1,7997	0,9986	0,0827	0,0522
	−500+425	5	1,0825	0,8685	0,9940	0,1614	0,1170	7	2,0656	1,5536	0,9969	0,1455	0,0880
Matla	−300+250	4	1,1488	0,9081	0,9988	0,0908	0,0671	9	2,1608	1,6128	0,9981	0,0945	0,0587
	−150+125	2	0,4991	0,3929	0,9993	–	–	10	2,2968	1,6878	0,9986	0,0787	0,0496
	−90+75	2	0,9956	0,7403	0,9993	–	–	9	2,4745	1,7916	0,9956	0,0802	0,0497
	−1000	12	2,0556	1,5668	0,9975	0,2277	0,1632						
	−500+425	2	0,8585	0,6835	–	–	–	14	2,0115	1,5697	0,9969	0,0403	0,0324
Waterberg	−300+250	2	0,5472	0,4436	–	–	–	14	1,9851	1,5507	0,9963	0,0215	0,1277
	−150+125	2	0,3687	0,3141	–	–	–	14	2,0036	1,5621	0,9922	0,0097	0,0254
	−90+75	2	0,4621	0,3797	–	–	–	14	2,0162	1,5753	0,9946	0,0034	0,0087

Notes: N and N1 are the number of points used to define the two straight lines on the plot of ash versus specific volume
A and A1 are the slopes, and B and B1 the intercepts of these lines

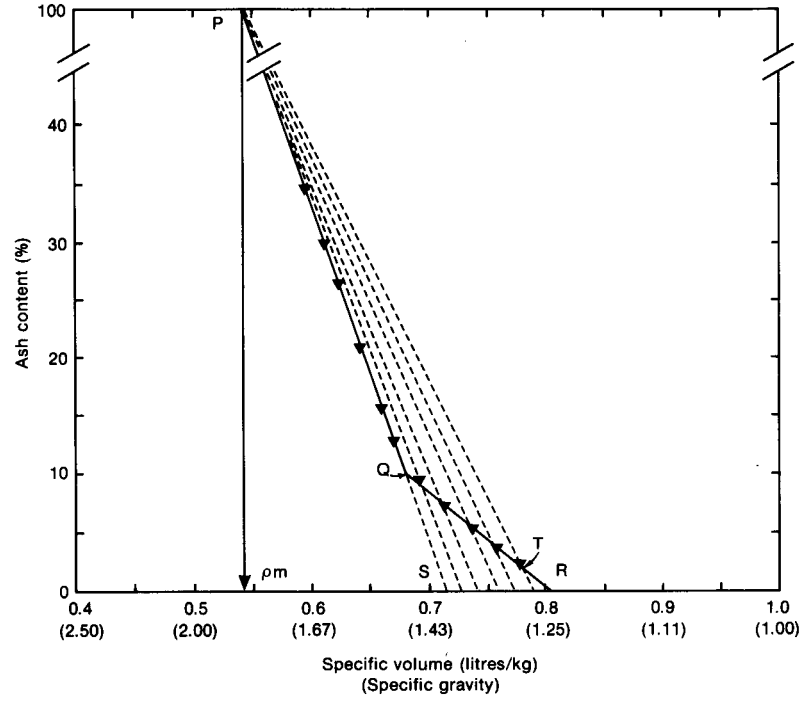

Fig. 5—Typical relationship between ash content and particle relative density. (The numbers in brackets give the relative densities.) The two straight lines are typical for all the coals investigated

TABLE VI
PARAMETERS IN EQUATION (8) FOR PERCENTAGE ASH AS A FUNCTION OF PARTICLE SPECIFIC VOLUME

Sample	Size μm	N	A	B	R	N1	A1	B1	R1	rd 1	Ash %	rd 5
Witbank N4 up	−425+300	5	−0,8182	0,6751	−0,9982	5	−2,7036	1,8696	−0,9901	1,578	10,97	2,59
Witbank N4 up	−38+25	7	−0,2322	0,2057	−0,9706	7	−3,3828	2,2174	−0,9938	1,566	4,50	2,32
Witbank N4 low	−425+300	7	−0,8854	0,7175	−0,9909	6	−2,5104	1,7488	−0,9956	1,576	9,36	2,79
Witbank N4 low	−38+25	3	−0,2042	0,1641	−0,9643	5	−2,7826	1,8773	−0,9981	1,505	1,00	2,64
Witbank N2 top	−425+300	6	−0,4097	0,3331	−0,9977	8	−2,9001	1,9701	−0,9938	1,521	4,66	2,49
Witbank N2 top	−38+25	3	−0,4676	0,3549	−0,9076	4	−2,5684	1,6993	−0,9970	1,563	1,95	3,06
Witbank N2 mid	−425+300	5	−0,5150	0,4114	−0,9949	8	−2,9547	2,0097	−0,9701	1,526	4,05	2,43
Witbank N2 mid	−38+25	3	−0,2489	0,2018	−0,5312	3	−2,2638	1,5448	−0,9941	1,500	1,47	3,46
Witbank N2 bot	−425+300	8	−0,6820	0,5402	−0,9957	4	−1,8539	1,2563	−0,9912	1,636	9,17	6,02
Witbank N2 bot	−38+25	6	−0,5736	0,4360	−0,9188	4	−3,5061	2,2973	−0,9783	1,576	5,84	2,25
Witbank N1	−425+300	7	−0,6606	0,5192	−0,9463	7	−2,6078	1,7880	−0,9991	1,535	6,97	2,75
Witbank N1	−38+25	2	−0,4403	0,3389	−0,9999	6	−2,3623	1,6087	−0,9992	1,514	1,05	3,23
Tshinkondeni	−1000+25	3	−1,0473	0,8411	−0,9808	8	−2,2256	1,7163	−0,9993	1,346	2,50	2,59
Tshinkondeni	−38+25	3	−1,0882	0,8587	−0,9723	6	−2,1254	1,6043	−0,9985	1,391	2,77	2,93
Secunda	−1000+25	7	−0,4629	0,3790	−0,9675	4	−2,2441	1,5120	−0,9986	1,572	7,00	3,65
Secunda	−38+25	6	−0,4487	0,3687	−0,9518	5	−2,0843	1,4175	−0,9956	1,559	6,33	4,16
Sigma N3	−425+300	6	−0,4512	0,3607	−0,9655	7	−2,7179	1,8181	−0,9961	1,555	5,54	2,77
Sigma N3	−38+25	6	−0,3962	0,3186	−0,7338	4	−2,9790	1,9186	−0,9995	1,614	7,64	2,70
Sigma 2A	−425+300	6	−0,5488	0,4378	−0,9794	6	−2,4928	1,6694	−0,9940	1,578	7,00	3,10
Sigma 2A	−38+25	3	−0,3133	0,2688	−0,6597	4	−2,5220	1,6735	−0,9999	1,572	4,60	3,12
Sigma 2B	−425+300	8	−0,9053	0,7151	−0,9564	4	−2,6549	1,7839	−0,9994	1,637	11,69	2,82
Sigma 2B	−38+25	5	−0,6141	0,4754	−0,6818	3	−2,8174	1,8690	−1,0000	1,581	6,46	2,70
Usutu B	−425+300	7	−1,1254	0,8823	−0,9976	5	−2,1449	1,5473	−0,9930	1,533	13,59	3,27
Usutu B	−38+25	5	−0,8014	0,6118	−0,9062	3	−2,4107	1,6188	−0,9991	1,598	10,01	3,24
Usutu C up	−425+300	8	−0,9322	0,7388	−0,9960	3	−2,5890	1,7471	−0,9993	1,643	14,39	2,89
Usutu C up	−38+25	3	−0,6173	0,4772	−0,9994	3	−2,5841	1,7221	−0,9999	1,580	5,31	2,98
Usutu C low	−425+300	7	−0,8647	0,6879	−0,9932	5	−2,4486	1,7188	−0,9976	1,536	9,51	2,84
Usutu C low	−38+25	5	−0,4303	0,3520	−0,9189	3	−2,4473	1,6702	−0,9859	1,530	5,94	3,04
Groot. N4	−425+300	2	−0,4136	0,3376	−1,0008	10	−2,0939	1,6200	−0,9994	1,310	1,30	2,81
Groot. N4	−38+25	4	−0,9068	0,6975	−0,9224	4	−2,2002	1,6341	−0,9993	1,381	1,82	2,89
Groot. N11	−425+300	2	−0,1418	0,1287	−0,9996	10	−2,0546	1,597	−0,9990	1,302	1,71	2,87
Groot. N11	−38+25	3	−0,2789	0,2350	−0,6008	5	−2,5268	1,8026	−0,9980	1,434	2,56	2,62
Groot. N18	−425+300	2	−0,2113	0,1787	−0,9920	11	−1,9235	1,5229	−0,999	1,274	1,24	3,07
Groot. N18	−38+25	5	−0,9456	0,7415	−0,8918	5	−2,5741	1,8494	−0,9988	1,470	9,19	2,52

Notes: N and N1 are the number of points used to define the two straight lines on the plot of ash versus specific volume
A and A1 are the slopes, and B and B1 the intercepts of these lines
R and R1 are the correlation coefficients
Ash and rd 1 are the coordinates of the break point in the plot
rd 5 is the calculated relative density of the mineral matter

become less dense (and lower in ash), the ratio of vitrinite to inertinite increases. The relative densities of vitrinite and inertinite in South African coals are estimated to be approximately 1,28 and 1,45 respectively (ref. 2, p. 59). These values correlate well with the range of intercepts for the broken lines on all the plots established in this study.

The two extreme points Q and T on the lower line represent the limiting ash content of the relatively pure inertinite and vitrinite macerals respectively. These points define the limiting ash content of these two macerals. In all the samples studied, there was more inherent ash in the inertinite than in the vitrinite, and in general the ash decreased with decreasing particle size (Tables V and VI).

Maceral Washability and Release

The analysis presented in the previous section provides evidence that a certain degree of inter-maceral liberation does occur at the particle sizes investigated, and that the macerals were separating from one another at the liquid densities used in the float-and-sink procedure. Such direct maceral liberation can be important technically because separation apparently occurs over the density ranges that can be implemented in industrial washing operations.

Direct observations of the maceral liberation were made by petrographic analysis of the individual fractions obtained during the float-and-sink investigation. Individual fractions were carefully mounted and polished, and maceral fractions were determined by the point-counting method. All the necessary precautions required to ensure accurate and reproducible results were taken. A very high level of skill is required for the petrographic analysis of coal, and the techniques used were compared with results obtained at the Iscor petrographic laboratory on a stan-

TABLE VII

MACERAL WASHABILITY AND RELEASE DATA FOR SAMPLE 9 (WITBANK NO. 2 SEAM TOP −425+300 μm FRACTION)

			Vitrinite				Inertinite				Exinite				Minerals			
Mean sepn rd	Vol frac %	Cum vol %	Grad† %	Rec %	Cum rec %	Per 100 units*	Grad† %	Rec %	Cum rec %	Per 100 units*	Grad† %	Rec %	Cum rec %	Per 100 units*	Rad† %	Rec %	Cum rec %	Per 100 units*
1,280	0,7	0,7	96,0	2,1	2,1	0,0222	3,0	0,0	0,0	0,0130	1,0	0,2	0,2	0,2381	1,0	0,1	0,1	0,0818
1,322	3,0	3,7	96,0	8,9	11,0	0,1150	3,0	0,2	0,2	0,0677	2,0	2,0	2,2	1,2364	1,0	0,3	0,4	0,4247
1,360	1,7	5,4	86,0	4,5	15,5	0,1671	10,0	0,3	0,5	0,0984	3,0	1,7	3,9	1,7962	3,0	0,6	1,0	0,6171
1,398	5,3	10,7	72,0	11,7	27,2	0,3293	23,0	2,2	2,7	0,1939	4,0	7,0	10,9	3,5403	3,0	1,8	2,8	1,2162
1,438	5,7	16,4	53,0	9,2	36,4	0,5034	40,0	4,1	6,8	0,2964	3,0	5,6	16,5	5,4112	4,0	2,6	5,4	1,8589
1,475	20,4	36,8	39,0	24,5	60,9	1,1309	52,0	19,2	26,0	0,6659	3,0	20,2	36,7	12,1563	5,0	11,6	17,0	4,1760
1,513	34,8	71,6	25,0	26,8	87,7	2,2014	66,0	41,6	67,6	1,2963	4,0	46,0	82,8	23,6640	6,0	23,7	40,7	8,1292
1,559	15,8	87,4	16,0	7,8	95,4	2,6860	73,0	20,8	88,5	1,5817	2,0	10,4	93,2	28,8736	7,0	12,5	53,2	9,9188
1,601	2,9	90,3	11,0	1,0	96,4	2,7745	69,0	3,6	92,1	1,6338	2,0	1,9	95,1	29,8251	18,0	5,9	59,1	10,2457
1,631	3,2	93,5	13,0	1,3	97,7	2,8730	69,0	4,0	96,1	1,6918	2,0	2,1	97,2	30,8836	16,0	5,8	64,9	10,6093
1,669	1,9	95,4	15,0	0,9	98,6	2,9324	64,0	2,2	98,3	1,7268	2,0	1,3	98,5	31,5225	19,0	4,2	69,1	10,8288
1,736	1,2	96,6	20,0	0,7	99,3	2,9678	53,0	1,1	99,4	1,7476	1,0	0,4	98,9	31,9026	25,0	3,3	72,3	10,9594
1,889	0,5	97,1	28,0	0,4	99,7	2,9828	30,0	0,3	99,7	1,7565	1,0	0,2	99,0	32,0639	41,0	2,3	74,6	11,0148
2,233	1,0	98,1	8,0	0,3	99,9	3,0145	16,0	0,3	100,0	1,7752	1,0	0,3	99,4	32,4050	76,0	8,9	83,5	11,1320
2,734	1,9	100,0	1,0	0,1	100,0	3,0733	1,0	0,0	100,0	1,8098	1,0	0,6	100,0	33,0364	76,0	16,5	100,0	11,3489
Total (measured)			29,0				59,0				2,0				10,0			
Total (calculated)			32,6				55,5				3,0				8,9			

Notes: * Per 100 units of feed

† Volumetric grade as determined from point counts. All grades are estimated to be correct to ±4%; decimals appear only for convenience

dard set of samples. The Iscor analysis can safely be assumed to be an absolute standard.

The volume fractions of vitrinite, inertinite, exinite, and mineral matter were determined in the mounted particulate samples. It was not considered appropriate to attempt a more detailed petrographic analysis, and only the three group macerals mentioned above were counted. Complete details of the procedures used can be found in Reference 2. Typical results from some samples are presented in Table VII.

The cumulative recoveries of the macerals and mineral matter from one sample are shown graphically in Figs. 6 to 8. The specific volume rather than the density is used as the abscissa in these plots to facilitate comparison with the plots of ash versus specific volume plots that were discussed earlier. As the relative density of separation increases (moving from right to left in Figs. 6 to 8), it is clear from all the graphs that the vitrinite is recovered first into the lightest fractions. This is generally followed by exinite and then inertinite although, in the coal from Grootegeluk, the exinite tended to follow the inertinite. Since the exinite is expected to have a lower density than the vitrinite, it is the association with the mineral matter rather than the inherent density of the maceral that determines the order of recovery.

The relevant percentage ash versus specific volume for each sample is shown in Figs. 6 to 8 so that this can be compared directly with the maceral recovery.

The three coals presented in Figs. 6 to 8 are representative of the three types of behaviour that were observed during this study. In the case of Witbank No. 2 seam (Fig. 6), the curves showing maceral recovery are very steep and not well separated. The coal from Grootegeluk (Fig. 8) showed the opposite characteristic, with all three macerals appearing comparatively slowly in the float fraction as the relative density of separation increased. The coal from the Eastern Transvaal coalfield (Fig. 7) showed a comparatively slow recovery of vitrinite with a rapid recovery of exinite and inertinite. This coal revealed a significant difference in relative density for the recoveries of vitrinite on the one hand, and exinite and inertinite on the other. The Eastern Transvaal coal appeared to be the most representative of all the coals studied, with the other two representing the extreme behaviour on either side.

The results for the Eastern Transvaal coal apparently confirm the mechanism proposed in the previous section to explain the break in the plots for percentage ash versus specific volume. The lower line is evidently associated with the progressive recovery of heavier and heavier combinations of vitrinite–inertinite mixtures, the break point occurring when the recovery of the lighter vitrinite is substantially complete. The upper line is associated with the successive recovery of progressively denser mixtures of inertinite and mineral matter. The results for the Witbank coal can also be explained on this basis but, although the break point is well-defined, there is a less clear-cut separation of the two macerals. The Grootegeluk coal appears to have a radically different characteristic. Here the break point is not well defined and is situated at a comparatively low relative density. This appears to be due to the rather more gradual recovery of all the macerals as the separation density increases.

Coal Cleaning and Separation of Macerals by Washing

The results obtained in this study make it possible to calculate directly the complete composition of the products from an ideal washing plant. This is illustrated by the results for the minus 1000 plus 245 μm fraction from Secunda. The results are summarized in the composite

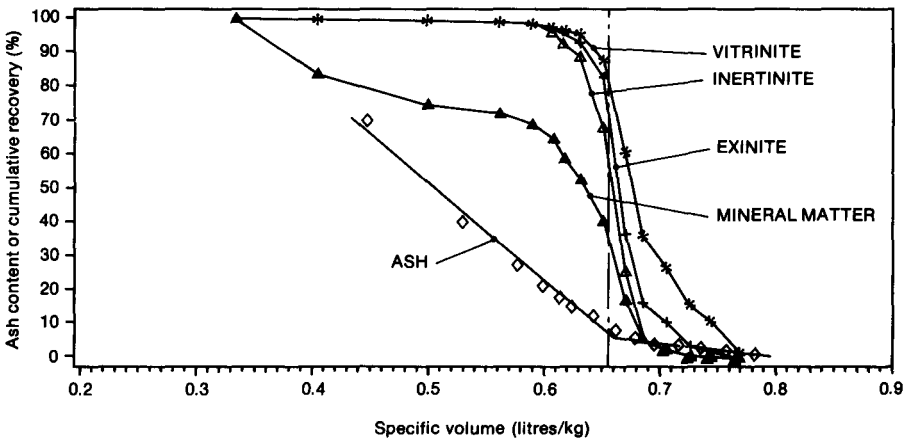

Fig. 6—Cumulative recovery of macerals superimposed on the plot for ash content versus specific volume. The vitrinite is almost all concentrated in the fractions associated with the lower straight line. Witbank No. 2 seam coal −425 +300 μm size fraction

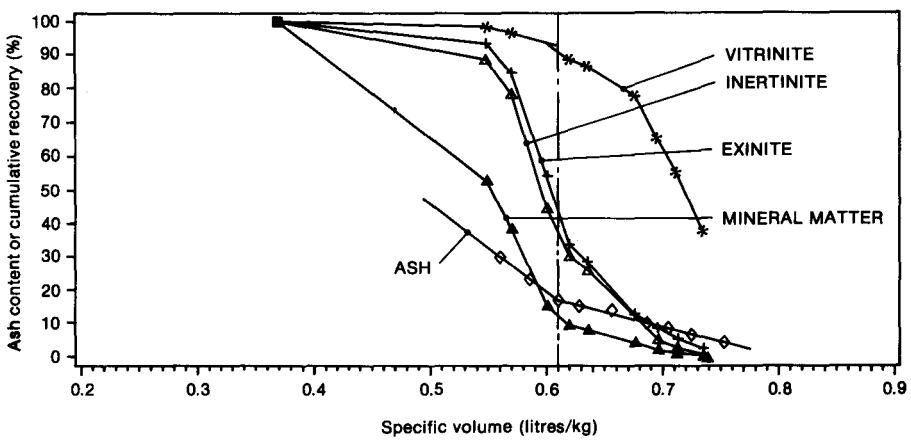

Fig. 7—Cumulative recovery of macerals superimposed on the plot for ash content versus specific volume. Almost all of the vitrinite is recovered into the low-density fractions associated with the lower straight line on the plot for ash content versus specific volume. Eastern Transvaal coalfields (Usutu seam C upper) −425 +300 μm size fraction

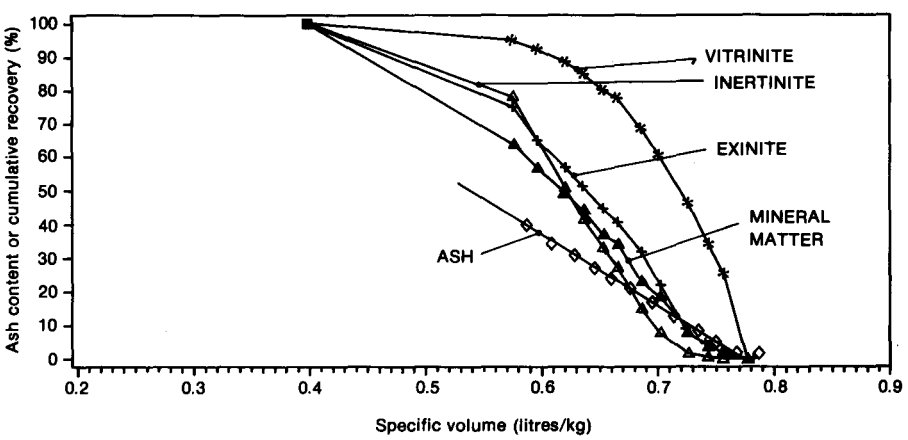

Fig. 8—Cumulative recovery of macerals superimposed on the plot for ash content versus specific volume. For this coal the vitrinite is distributed with the other macerals over almost the entire range of density fractions. Coal from the Waterberg coalfield (Grootegeluk No. 4) −425 +300 μm size fraction

Fig. 9, which includes the M-curve and the curves for percentage ash versus specific volume and for cumulative vitrinite recovery. Also shown is the release curve for vitrinite plotted in the usual manner.

Consider an ideal two-stage washing operation with the first stage cutting the feed at an instantaneous ash value of 7 per cent and a second stage set to produce a middlings fraction containing 12 per cent ash. The following graphical procedure allows the direct calculation from Fig. 9 of the separation density required in each stage, the ash content of the clean coal and final product, and the volumetric grade and recovery of vitrinite in each product. The calculation can also be done by the use of equations (1) to (5) and equation (8). The use of these equations is very useful for the implementation of the procedure by computer.

Data for the calculation:

% ash in the feed 18,7

Petrographic data: vitrinite 17,3%, inertinite 59,2%, exinite 2,9%, and mineral matter 20,5% (by volume)

Ash in terms of specific volume (equation (8) and Table VI)

$$\% \text{ ash} = -\frac{46{,}3}{rd} + 37{,}9 \text{ for relative density} \leqslant 1{,}57 \quad \ldots\ldots (9)$$

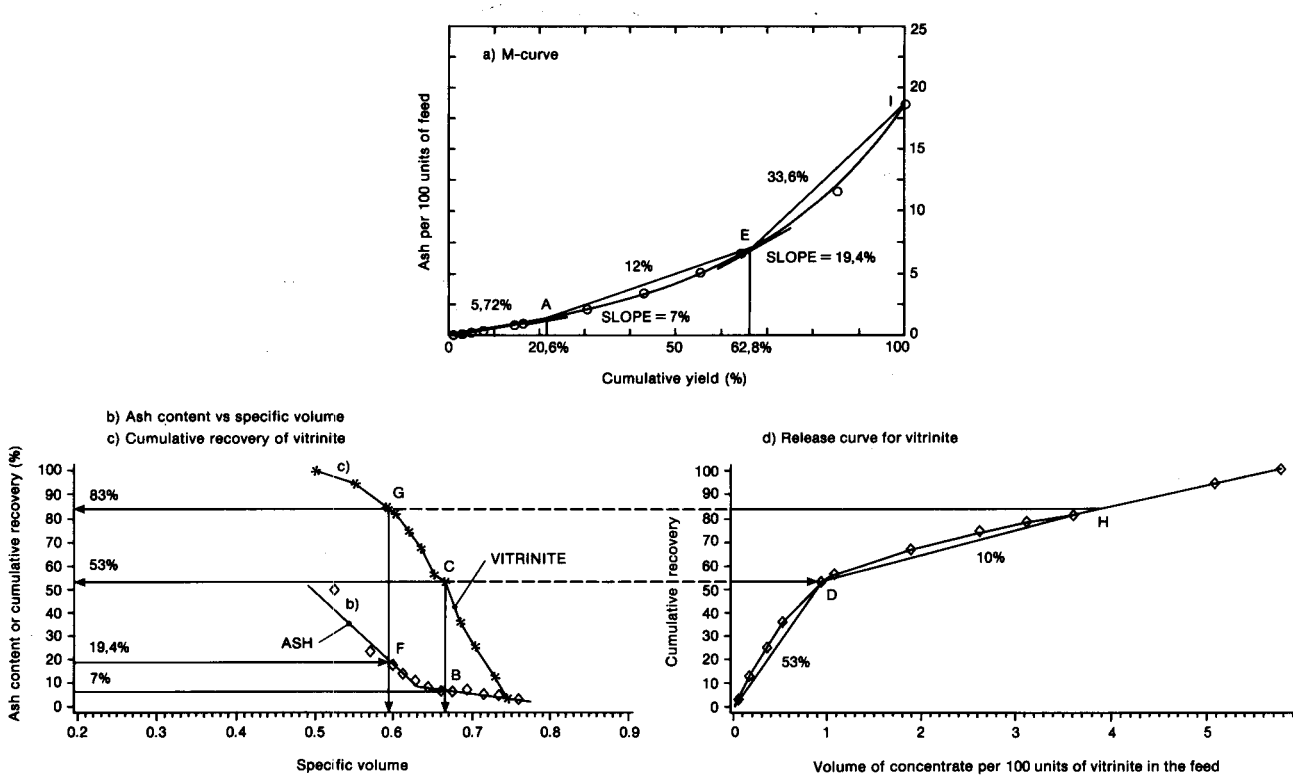

Fig. 9—Composite plots of data for the −1000 +25 μm composite fraction from Secunda. This composite plot can be used to evaluate the performance of any ideal multistage coal-washing plant as described in the text

$$\% \text{ ash} = -\frac{224,4}{rd} + 151,2 \text{ for relative density} \geqslant 1,57. \quad \ldots\ldots (10)$$

The equation of the M-curve (equation (1) and Table IV)

$$Z = 0,01933Q \exp(2,095Q) + 0,0274Q. \quad \ldots\ldots (11)$$

The cut point for the first washing stage is located on Fig. 9a at the point where the tangent has a slope of 7 per cent. This is shown at point A. This point can also be found by solving equation (4) with a_1 equal to 7 per cent, which gives a yield, Q, of 20,6 per cent. The cut point for the first stage is obtained from the curve for percentage ash versus specific volume (Fig. 9b) at point B or from equation (9):

$$\text{Cut point relative density} = \frac{46,3}{37,9 - 7} = 1,50$$

(specific volume = 0,667).

The ash content of the clean coal is given by the slope of line OA in Fig. 9a or from equation (3):

$$a_c = 0,01933 \exp(2,095 \times 0,206 + 0,0274 = 5,72 \text{ per cent.}$$

The recovery of vitrinite is obtained from curve 9c at point C, and is 53 per cent. The coal in the clean product will contain 53 per cent vitrinite by volume determined from the slope of line OD in Fig. 9d.

The cut point for the second stage is obtained by drawing line AE with a slope of 12 per cent on curve 9a. This can also be done analytically by solving

$$0,01933Q\exp(0,02095Q_1) + 0,0274Q_1 + 0,12(Q - Q_1) = 0,01933Q \exp(0,02095Q) + 0,0274Q, \quad \ldots\ldots (12)$$

where Q_1 is 20,6 per cent. The solution to equation (12) is Q = 62,8 per cent.

The instantaneous ash is given by the slope of the M-curve (Fig. 9a) at point E or by equation (4) as 19,4 per cent.

The cut point for the second stage is obtained from Fig. 9b at point F or from equation (10) as

$$\text{Cut point relative density} = \frac{224,4}{151,2 - 19,3} = 1,70$$

(specific volume = 0,588).

The recovery of vitrinite in the middlings is obtained from Fig. 9c at point G as (83 − 53) = 30 per cent, and the vitrinite content in the middlings is obtained from the slope of line DH in Fig. 9d and is 10 per cent by volume.

Finally, the ash content of the discards is obtained from the slope of EI in Fig. 9a. The discards contain 17 per cent of the total vitrinite in the feed.

The use of the M-curve and the release curves as described above gives the performance of an ideal washing plant that includes only perfect separation devices. In practice, it is impossible to realize such ideal separations, especially in the treatment of fine coal, since even the most effective washing device, the dense-medium cyclone, shows significant inefficiencies at fine sizes[7].

The results of this study are very useful in calculating the performance of actual operating plants, particularly when used with an effective plant simulator such as

MODSIM[8-10]. This computer system can simulate the performance of any mineral-processing plant, and excellent models for coal-washing equipment are incorporated in the simulator. In particular, the performance of dense-medium cyclones is very effectively modelled for fine coal washing. Details of this model are given in Reference 7. An example of the data for the Secunda sample required by the simulator are summarized in Tables VIII and IX.

TABLE VIII
SIZE DISTRIBUTION IN THE SECUNDA SAMPLE

Sieve size μm	Retained %	Ash (dry) %
850	3,2	17,5
600	23,2	18,4
500	9,3	19,7
425	11,5	18,9
300	13,2	18,9
250	5,4	18,8
212	3,3	18,6
150	9,2	18,8
125	2,5	19,0
106	4,0	19,2
90	1,1	18,4
75	1,7	18,6
53	4,3	19,0
38	0,9	17,6
25	1,0	18,5
-25	6,2	24,9

The simple two-stage washing plant shown in Fig. 10 was simulated for several combinations of the medium density in each dense-medium cyclone. The actual separation density will be above the preset medium density because of the significant shift in cut point that occurs when fine coal is washed in a dense-medium cyclone[8]. The non-ideal nature of the operation is modelled by use of an appropriate partition function, with the imperfection of a strong function of particle size[7].

These simulations showed clearly that it would not be possible to make a clean coal with 5,72 per cent ash as obtained by the ideal calculation procedure. Given the inherent inefficiency of the real washing process, it would not be possible to produce a clean coal from the Secunda sample at better than 8,5 per cent ash. The performance of the simulated plant at the ideal settings and conditions set to match the yield of clean coal and middlings is given in Table X.

The simulator calculates the behaviour of the macerals in the coal, as well as the ash, and the recovery of the three macerals and the maceral composition of the clean coal and middlings are shown in Table XI.

These calculation procedures demonstrate the usefulness of the washability and petrographic results for fine coals that are presented in this paper and in the project reports[3,4]. The results are sufficiently comprehensive to enable these calculations to be made for a wide selection of fine coals that are likely to be produced in South African collieries.

Conclusions

The washability characteristics of fine coal produced in South African collieries were characterized by use of very precise float-and-sink analyses. These characteristics can be usefully represented as M-curves. Perfect liberation of organic material cannot be achieved even at very fine sizes, and there are limiting ash contents for each of the most important macerals. However, an index of liberation can be defined by use of the geometry of the M-curve, and this index can be used to show the relative increase in liberation as the particle size decreases from minus 425 plus 300 μm to minus 38 plus 25 μm. The coals that were studied showed a wide variation in the percentage increase of the liberation indices between these two sizes. Coal from Sigma Colliery showed virtually no increase in the liberation index, while coal from the Witbank No. 2 seam showed a 29 per cent increase in the liberation index (Table IV).

A new relationship between the ash content of coal particles and their relative density was developed, and this could be well represented by two straight lines in the space representing ash content and specific volume. This representation is very useful for practical calculations,

TABLE IX
WASHABILITY AND PETROGRAPHY OF SECUNDA SAMPLE

rd of separation	Mean rd in interval	Ash %	Mass in interval %	Vitrinite by volume %	Inertinite by volume %	Exinite by volume %
1,344	1,322	2,74	0,6	85,7	9,5	2,7
1,375	1,359	3,89	1,7	79,8	20,9	2,0
1,424	1,399	4,50	2,8	64,3	26,4	4,0
1,463	1,443	6,84	2,6	61,1	27,8	4,5
1,503	1,4831	6,33	6,8	39,8	47,8	4,9
1,534	1,519	7,00	1,9	22,9	56,5	2,5
1,575	1,554	8,27	14,4	13,3	75,7	3,9
1,616	1,595	10,78	12,4	10,0	74,9	3,9
1,658	1,637	13,83	12,4	9,6	74,0	3,1
1,692	1,675	17,07	9,1	5,8	74,8	2,9
1,812	1,752	23,28	21,0	8,2	61,4	2,2
-1,812	1,906	49,76	14,3	8,6	27,6	0,2
Composite		18,75		16,2	59,1	2,8

rd = Relative density

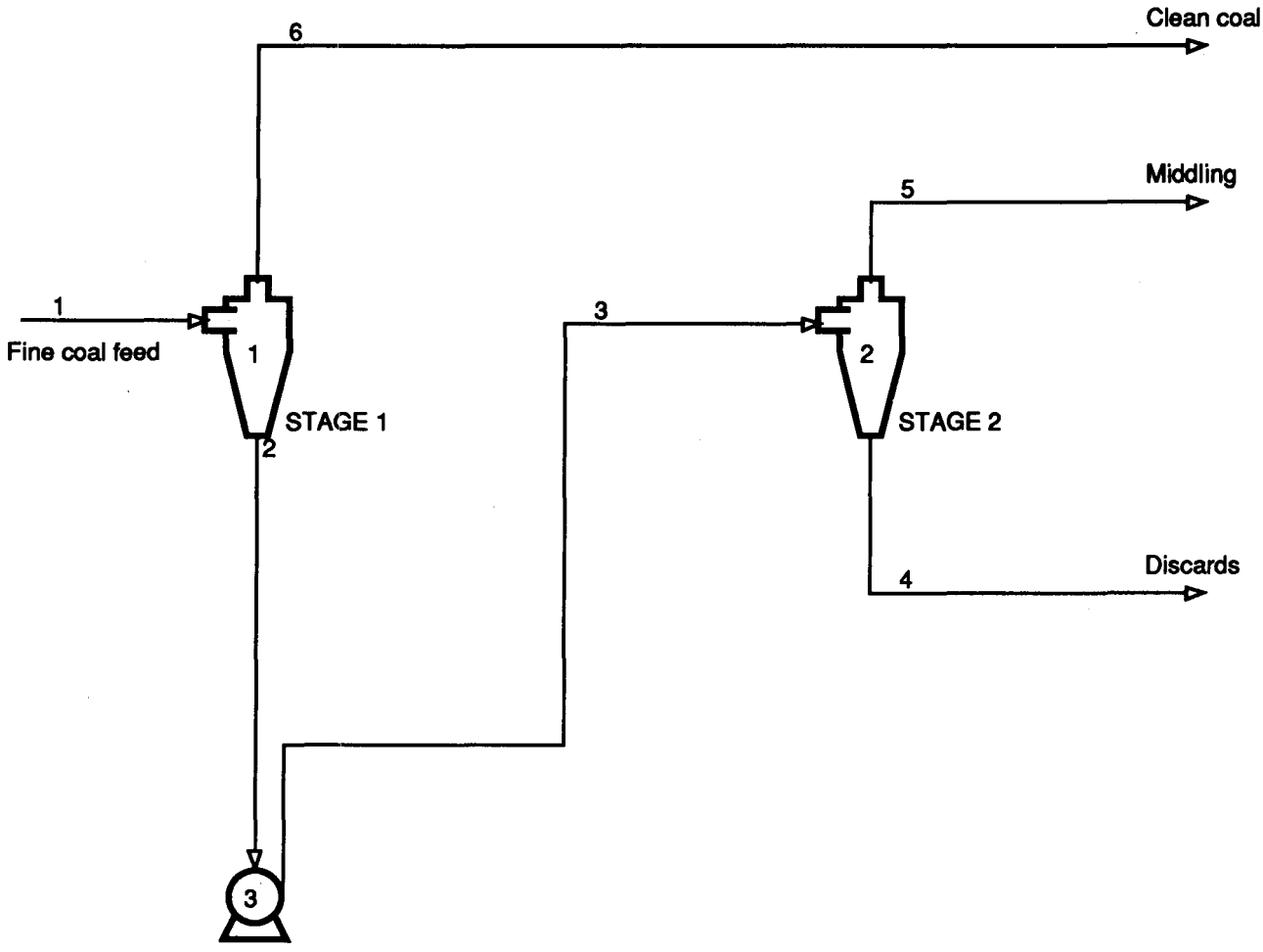

Fig. 10—Simple two-stage process used to simulate the real behaviour of a typical fine-coal washing plant

TABLE X
SIMULATED PERFORMANCE OF A TWO-STAGE DENSE-MEDIUM CYCLONE CIRCUIT PROCESSING THE SECUNDA SAMPLE

Calculation procedure	Medium density		Yield of clean coal %	Yield of middlings %	Ash in clean coal %	Ash in middlings %	Ash in discards %
	Stage 1	Stage 2					
Ideal (Fig. 9)	1,50	1,70	20,6	42,2	5,72	12,0	13,6
MODSIM Simulation 1	1,50	1,70	38,1	44,3	9,56	17,9	40,8
MODSIM Simulation 2	1,42	1,59	20,6	42,0	8,75	12,8	30,8
MODSIM Simulation 3	1,42	1,55	20,6	33,1	8,75	12,0	28,1

Notes: Simulation 1 Same medium density settings as for the ideal case
Simulation 2 Medium densities in each stage set to match the yield of clean coal and middlings predicted by the ideal procedure of Fig. 9
Simulation 3 Medium densities set to match the yield of clean coal and ash content in the middlings predicted by the ideal procedure of Fig. 9

TABLE XI
RECOVERY AND GRADE OF MACERALS IN THE PRODUCTS OF THE SIMULATED TWO-STAGE PLANT

Calculation procedure	Maceral recovery in clean coal			Vol % maceral in clean coal			Vol % maceral in middling		
	Vitrinite	Inertinite	Exinite	Vitrinite	Inertinite	Exinite	Vitrinite	Inertinite	Exinite
Ideal	53			53			10		
MODSIM Simulation 1	65	38	50	28	58	4	9	68	3
MODSIM Simulation 2	48	17	27	37	49	4	13	70	3
MODSIM Simulation 3	48	17	27	37	49	4	14	70	4

and can be interpreted in terms of inter-maceral liberation and the varying limiting ash content of the different macerals.

The results obtained during this study and their interpretation as developed in this paper permit the accurate calculation of product yields, together with mineral matter, and the ash and maceral contents of the products, from any ideal multistage coal-washing operation. The results can also be supplied to an accurate and reliable simulator such as MODSIM to give accurate calculations of the expected performance of any real plant. These simulations show that the low ash content in the clean coal as predicted by the ideal calculation procedure cannot be achieved in any real plant, thus emphasizing the need for accurate calculation procedures that make allowance for the imperfect separation that is characteristic of real coal-washing operations.

Acknowledgements

This project was undertaken with support of the Cooperative Scientific Program of the CSIR (later the National Energy Programme of the Foundation for Research Development). Support was also provided by Van Eck & Lurie. This support is very gratefully acknowledged. Extensive and exceedingly valuable assistance was provided by Mr W. Smith and his assistants at Iscor. Assistance and facilities for the collection of samples were provided by BP South Africa, Gencor, Iscor, Sasol, and Anglo American Corporation. These are gratefully acknowledged. Miss C. Dixon, Mr S. Moqabolane, and Miss D. Tao assisted with the precise float-and-sink analyses and the ash determinations.

References

1. FALCON, R. Petrographic characterisation of coals from the No. 2 seam, Witbank Coalfield. Johannesburg, Bureau for Mineral Studies, University of the Witwatersrand, 1981. pp. 18–52.
2. BIRTEK, N. Liberation characteristics of South African coals in the size range − 1000 + 25 μm. Johannesburg, University of the Witwatersrand, MSc thesis, 1987. 429 pp.
3. BIRTEK, N., and KING, R.P. Distribution of ash in fine coal from several South African collieries. Johannesburg, Dept of Metallurgy and Materials Engineering, University of the Witwatersrand, *Report* CSPCOAL-5, 1984. 151 pp.
4. BIRTEK, N., and KING, R.P. Distribution of ash in fine coal from several South African coalfields. Johannesburg, Dept of Metallurgy and Materials Engineering, University of the Witwatersrand, *Report* CSPCOAL-14, 1986. 165 pp.
5. JOWETT, A., and SMITH, H.W. Calculations related to flotation in an optimized coal cleaning system. *Can. Metall. Q.*, vol. 25. 1986. pp. 91–99.
6. JOWETT, A. Formulae for the technical efficiency of mineral separations. *Int. J. Miner. Process.*, 1975. pp. 287–301.
7. KING, R.P., and JUCKES, A.H. Performance of a dense-medium cyclone when beneficiating fine coal. *Coal Preparation* no. 5. 1988. pp. 185–210.
8. KING, R.P. MODSIM: A method for the design, balancing and simulation of ore dressing plant flowsheets. Johannesburg, Dept of Metallurgy, University of the Witwatersrand, *Report* G9, 1983. 51 pp.
9. KING, R.P. A user's guide to MODSIM. Johannesburg, Dept of Metallurgy and Materials Engineering, University of the Witwatersrand, *Report* GEN/1/86. 1986. 63 pp.
10. FORD, M.A., and KING, R.P. Simulation of ore dressing plants. *Int. J. Miner. Process.*, vol. 12. 1984. pp. 285–304.

Recycling of refrigerants*

Thousands of kilograms of ozone-depleting CFC (chlorofluorocarbon) gases continue to be dumped into the atmosphere annually by the refrigeration and air-conditioning industry, making it the second-largest single contributor to destruction of the ozone layer. However a new service that is now being offered to the market will prevent the freeing of CFCs from refrigerators and air conditioners during repairs.

Mr Larry Symington, owner of recently formed Refrigerant Reclaim Services, explained: 'Because of the historically cumbersome procedures involved in decanting CFC gases during repairs to refrigerators and air conditioners, these are currently simply released into the air and replaced by new gas'. He added that, while much attention was being directed to the need for limiting the use of aerosols, few people realized the extent of the contribution by the refrigeration and air-conditioning industry to ozone depletion.

In conjunction with the Wildlife Society of Southern Africa, which has long pioneered for a reduction in the use of CFCs, Mr Symington has embarked on a campaign to educate both users and repair contractors in combating the CFC problem until alternative chemical solutions can be found. 'The secret lies in recycling: in recovering the gas during repairs and storing it for re-use', said Mr Symington.

Initially, he was prepared to import a recovery station from the UK, with which he intended to provide a recycling service to the industry. This station has several advantages over previous designs, being compact and totally portable. Another innovation is that gas can now be condensed into liquid form within the unit itself, thereby eliminating the need for additional equipment and complex procedures.

'However, I soon discovered that it was feasible to copy that equipment and make my own station. With this pilot system, I have already successfully decanted gas from an air-conditioning system at Pretoria's Menlin Park Shopping Centre, while orders are beginning to flow in for several more jobs', reported Mr Symington.

The first phase in creating awareness will be directed at repair contractors, who are active at the forefront of the issue. Mr Symington has sponsored a seminar on the subject, which is to be held on 29th November, 1990, in Midrand. Speakers will include well-known campaigner for conservation of the environment, Mr Laurie Smith, who is chairman of the Pretoria Centre of the Wildlife Society of Southern Africa. Among the other speakers is Mr Danny Vann of AECI, and Mr Brian Huntley of the CSIR, co-author with Clem Sunter on *SA Environment in the 21st Century*.

The seminar will be followed by a presentation early in the new year under the auspices of SAIRAC, the South African Institute for Refrigeration and Air Conditioning.

* Released by Maggie Monsieur Communications, P.O. Box 93, Halfway House, 1685 Transvaal.

Permitted explosives*

The SABS Permit to apply the SABS diamond-ellipse standardization mark to permitted explosives and the SABS Listing Certificate were awarded recently to AECI Explosives & Chemicals Limited's Packaged Explosives Department. These have been extended to cover the Company's POWERGEL® emulsion permitted explosive.

Dr J.P. du Plessis, Director General of the SABS, handing the SABS Permit and Listing Certificate for POWERGEL® emulsion explosive to Mr J.E. Coetzee, Production Director, AECI Explosives & Chemicals Limited

* Released by AECI Explosives and Chemicals Limited, P.O. Box 1122, Johannesburg 2000.

AECI Explosives & Chemicals Limited is the first company in South Africa to attain the SABS standardization mark for emulsion explosives, and the only company to be awarded the SABS mark for all its permitted explosives.

With this powerful mark of recognition, POWERGEL® permitted explosive now joins the Company's other explosives products, i.e. AJAX® permitted and COALEX® permitted, which were awarded the SABS standardization mark for permitted explosives in August 1989.

The benefits to customers buying an explosive that bears the SABS mark are twofold:

- All products are manufactured and tested in accordance with the stringent requirements specified in the permit conditions, and they are sampled and tested regularly by the SABS for compliance with the safety and performance requirements of the specification for permitted explosives.
- The mark ensures a more reliable product with a higher standard of safety.

Addressing the employees of Packaged Explosives, SABS Director General, Dr J.P. du Plessis, commended the department on its high standard of quality production. 'Quality is everybody's business', he said, 'not just company directors' or managers' '. Achieving the SABS mark, he said, would create a domino effect—the effect of creating confidence throughout the company. 'You will all now be seeking and maintaining quality for the right reasons'.

Boet Coetzee, E&C's Production Director, informed the assembled plant managers and employees that Modderfontein had decided to put the whole factory on the scheme of SABS listing. 'It may be a painful process', he said, '. . . but we believe in it because the benefits far outweigh the costs'.

Advanced mining and processing

Papers are invited for Kaivos '91, which is to be held in Helsinki (Finland) from 2nd to 4th June, 1991.

As the worldwide mining industry begins this century's last decade, this important international Symposium will examine practical examples of Tomorrow's Mine and Plant Practice, and demonstrate, through operating experience, How to Cut Costs, Improve Productivity, and Increase Safety.

Kaivos '91 will be a truly international event, drawing on speakers and attendees from all around the world. It is being organized under the auspices of the Finnish Institution of Mining Engineers, and support has been promised by other professional mining institutions and societies in Europe and North America.

The Organizing Committee has already begun the process of paper selection for this Symposium. Engineers interested in submitting papers are invited to send or fax 300–500 word abstracts by 21st September, 1990, to

Kaivos '91
Prof. Raimo Matikainen
The Finnish Association of Mining and Metallurgical Engineers
Vuorimiehentie 2A
SF-02150 Espoo
Finland.
Telefax: +358 0451 2660.

The Committee is looking for presentations that show how the latest advances in mining, processing, or metallurgical technology and equipment have been implemented in practice, and the benefits that these innovations have generated. Papers should concentrate on

- Productivity
- Efficiency
- Safety
- Economy.

The Symposium will be followed by excursions to examples of advanced mining technology in the Nordic Region—an area that has long been at the forefront of imaginative and highly successful developments in equipment and technology.